INTERNATIONAL JOURNAL OF PRECISION ENGINEERING AND MANUFACTURING-GREEN TECHNOLOGY Vol. 2, No. 3, pp. 299-303 JULY 2015 / 299
DOI: 10.1007/s40684-015-0036-5 ISSN 2288-6206 (Print) / ISSN 2198-0810 (Online)

Effect of Inductance in Micro EDM Using High Frequency Bipolar Pulse Generator

Do Kwan Chung[1,#] and Chong Nam Chu[2,#]

1 School of Robot and Automation Engineering, Dongyang Mirae University, 445 Gyeongin-ro, Guro-gu, Seoul, 152-714, South Korea
2 School of Mechanical and Aerospace Engineering, Seoul National University, 1 Gwanak-ro,Gwanak-gu, Seoul, 151-015. South Korea
Corresponding Author / E-mail: dkchung@dongyang.ac.kr, TEL: +82-2-2610-5186, FAX: +82-2-2610-1852
E-mail: cnchu@snu.ac.kr, TEL: +82-2-880-7147, FAX: +82-2-887-7259

KEYWORDS: Micro EDM, High frequency bipolar pulse, Effect of inductance, Deionized water

In this work, effect of inductance was investigated in micro EDM using high frequency bipolar pulse generator used for electrolytic corrosion prevention in deionized water. To understand behaviors of the pulses during machining according to inductance, capacitor voltage which is equal to gap voltage and inductor current were analyzed both theoretically and experimentally. Inductance affected the pulse behaviors as well as machining characteristics. In the case of high inductance, inductor current increased after discharge occurred. This increased inductor current also increased both capacitor voltage and discharge current. So, machining time decreased, and tool wear as well as side gap increased with high inductance. However, this peak value shift could lead fluctuation of gap distance and servo voltage, thus, deteriorated controllability. On the other hand, constant discharge current was achieved in the case of low inductance. Low tool wear, small side gap and fine surface were achieved with low inductance.

Manuscript received: February 22, 2015 / Revised: April 16, 2015 / Accepted: April 24, 2015

1. Introduction

Micro EDM is a very attractive method to produce micro molds or precision parts in various industries.[1,2] In micro EDM, dielectric fluid plays an important role. As a dielectric fluid, deionized water is widely used because it leads high machining rate and low tool wear.[3] However, machined products suffer from electrolytic corrosion resulting in poor accuracy. To overcome this problem, deionized water usually used to machine workpiece materials with high resistance to corrosion such as stainless steel.[3] When the workpiece material is tungsten carbide (WC-Co) which is easily damaged due to electrolytic corrosion, bipolar pulse with RC circuit and special shaped tool were adopted to reduce corroded area.[4] To prevent electrolytic corrosion completely on tungsten carbide material, high frequency bipolar pulse generator was developed.[5,6] The generator and the open gap voltage is shown in Fig. 1. The generator is composed of single switch (MOSFET) and RLC components. High and narrow positive voltage and successive low and long negative voltage is provided to the machining gap. Using this generator, corrosion free micro features was fabricated successfully with high machining rate and low tool wear. Machining characteristics and theoretical studies were conducted about this generator. However, analysis of inductance effect which is one of important circuit components in the generator was not conducted yet. In this study, effect of inductance of the high frequency bipolar pulse generator on the

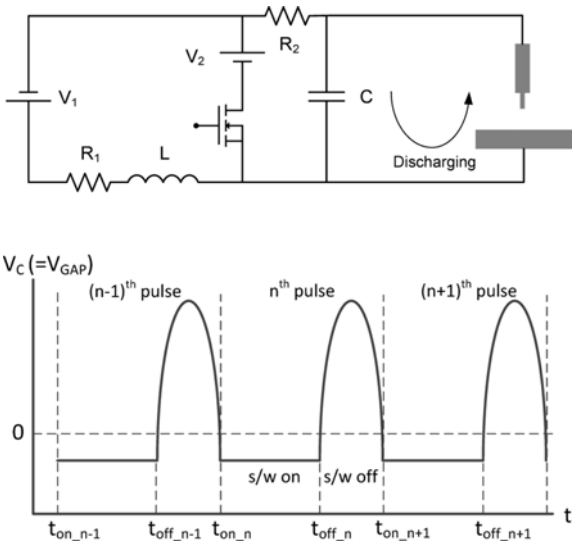

Fig. 1 High frequency bipolar pulse generator of micro EDM used in this study and capacitor voltage (=gap voltage)

machining characteristics is analyzed.

2. Analysis of Capacitor Voltage and Inductor Current of High Frequency Bipolar Pulse Generator

2.1 Switch On Mode

Fig. 2 shows the equivalent circuit when the switch is turned on. When the switch is turned on, a voltage across the switch is zero. A voltage supplied by DC power source (V_2) is formed across a capacitor. Therefore, negative voltage is provided to the machining gap. Considering n^{th} pulse, following first-order differential equations are given from the left and right mesh, respectively.

$$\frac{di_L}{dt}+\frac{R_1}{L}i_L=\frac{V_1+V_2}{L} \tag{1}$$

$$\frac{dV_C}{dt}+\frac{V_C}{R_2C}=-\frac{V_2}{R_2C} \tag{2}$$

where i_L and V_C are the inductor current and capacitor voltage (gap voltage), respectively. The solution is in the form of

$$i_L(t)=\frac{V_1+V_2}{R_1}+\left[i_L(t_{on\_n})-\frac{V_1+V_2}{R_1}\right]e^{-\frac{(t-t_{on\_n})}{L/R_1}} \tag{3}$$

$$V_C(t)=-V_2+[V_C(t_{on\_n})+V_2]e^{-\frac{(t-t_{on\_n})}{R_2C}} \tag{4}$$

The inductor current and the capacitor voltage have a transient response in the form of exponential function and a forced response with the value of $(V_1+V_2)/R_1$ and $-V_2$, respectively. When the time constant ($\tau = L/R_1$ and R_2C) is small, the inductor current and capacitor voltage reach their forced responses in a very short time. In case of $R_2 = 4.7\ \Omega$ and C = 390 pF, which were used in actual experiment, the time constant of the capacitor voltage is $\tau = 1.8$ ns. Since the time duration for switch on which is denoted by negative time is several hundreds of nanoseconds in actual experiment, the capacitor voltage can be considered as its forced response during switch on time ($V_C(t)=-V_2$).

2.2 Switch Off Mode

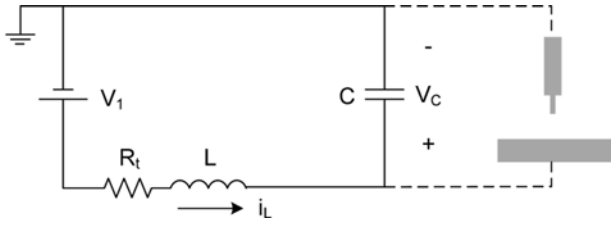

Fig. 2 Equivalent circuit when the switch is turned on

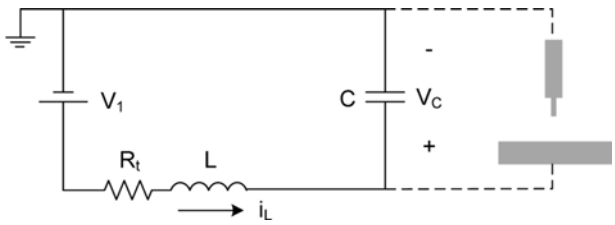

Fig. 3 Equivalent circuit when the switch is turned off ($R_t = R_1 + R_2$)

When the switch is turned off, the DC power source (V_2) is disconnected and the equivalent circuit forms a series RLC circuit as shown in Fig. 3. R_t is a sum of R_1 and R_2 ($R_t = R_1 + R_2$). The series RLC circuit gives a second-order differential Equation in a form of

$$\frac{d^2V_C}{dt^2}+\frac{R_t}{L}\frac{dV_C}{dt}+\frac{1}{LC}V_C=\frac{V_1}{LC} \tag{5}$$

In order to make oscillating wave, the circuit should be underdamped. If $\omega_n^2>\alpha^2$, the circuit is underdamped, where damping constant is $\alpha=R_t/2L$, and resonant frequency is $\omega_n=1/\sqrt{LC}$. The underdamped response is

$$V_C(t)=e^{-\alpha(t-t_{off\_n})}\{A_1\cos\omega_d(t-t_{off\_n})+A_2\sin\omega_d(t-t_{off\_n})\}+V_1 \tag{6}$$

And the damped resonant frequency is denoted by

$$\omega_d=\sqrt{\omega_n^2-\alpha^2}=\sqrt{\frac{1}{LC}-\frac{R_t^2}{4L^2}} \tag{7}$$

The inductor current is given by

$$i_L(t)=Ce^{-\alpha(t-t_{off\_n})}\{(\omega_dA_2-\alpha A_1)\cos\omega_d(t-t_{off\_n}) -(\omega_dA_1+\alpha A_2)\sin\omega_d(t-t_{off\_n})\} \tag{8}$$

The two coefficients A_1 and A_2 are determined by initial conditions. Because the voltage across a capacitor and the current in an inductor cannot change instantaneously, the capacitor voltage and the inductor current at the end of previous mode (switch on mode) are initial conditions, and they are denoted as $V_C(t_{off\_n})$ and $i_L(t_{off\_n})$, respectively. Therefore, two coefficients are

$$A_1=V_C(t_{off\_n})-V_1 \tag{9}$$

$$A_2=\frac{1}{\omega_d}\left[\frac{i_L(t_{off\_n})}{C}+\alpha\{V_C(t_{off\_n})-V_1\}\right] \tag{10}$$

Fig. 4 shows the simulated oscillating voltage across the capacitor at switch off mode where $R_1 = 17\ \Omega$, $R_2 = 4.7\ \Omega$, L = 4.5 μH,

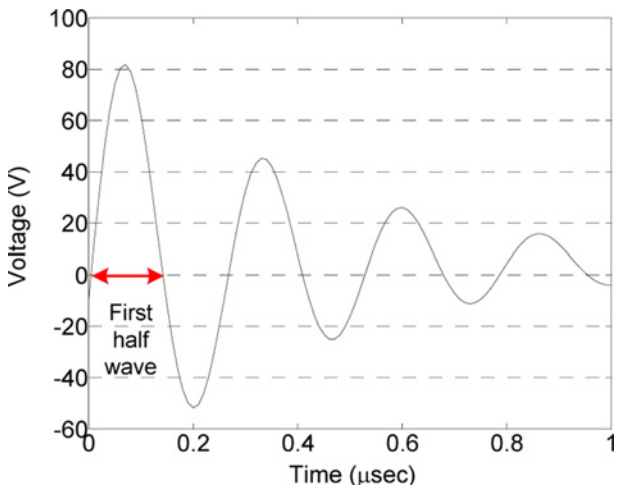

Fig. 4 Oscillating capacitor voltage of series RLC circuit for switch off mode ($R_1 = 17\ \Omega$, $R_2 = 4.7\ \Omega$, L = 4.5 μH, C = 390 pF, $V_1 = 4.5$ V, $V_2 = 10$ V)

C = 390 pF, V_1 = 4.5 V and V_2 = 10 V. The initial time is assumed to zero ($t_{off\_n} = 0$). The initial conditions at switch off mode used in the simulation are

$$V_C(t_{off\_n}) = V_C(0) = -V_2 \tag{11}$$

$$i_L(t_{off\_n}) = i_L(0) = \frac{V_1 + V_2}{R_1} \tag{12}$$

where the initial condition of inductor current is assumed to the forced response at previous mode. The oscillating voltage increases 80 V that is suitable for micro EDM and goes to the steady state value of 4.5 V. The first half wave (denoted by the arrow) is used for machining and the switch is turned on at the end of first half wave. Fig. 5(a) shows the capacitor voltage when the switch is turned on at the end of first half wave of oscillating voltage. Fig. 5(b) shows the capacitor voltage when the switch is turned on after the first half wave. Voltage pulse shown in Fig. 5(a) is preferable because the high repetition rate is attainable while maintaining average open gap voltage (with no discharges) is zero for corrosion prevention.[5,6]

3. Experiment

Table 1 shows experimental conditions. Tool material was tungsten carbide and its diameter was 100 μm. Workpiece material was also tungsten carbide and its thickness was 200 μm. Dielectric fluid for micro EDM was deionized water. The circuit component values were positive voltage = 80 V, R_1 = 17 Ω R_2 = 4.7 Ω C = 390 pF and repetition frequency = 1 MHz. Negative voltage was determined, so that the average open gap voltage (with no discharges) became zero. The inductance values were cable inductance, 0.5, 4.5, 10 and 22 μH. In the case of 22 μH, R_2 = 100 Ω were used for stable electrical short detection during machining.

Micro holes were drilled by micro EDM to evaluate machining characteristics according to inductance values. Drilling feedrate was in the range of 2~10 μm/s. Maximum feedrate of 10 μm/s was determined because higher feedrate can break the tool when the electrical short occurs.

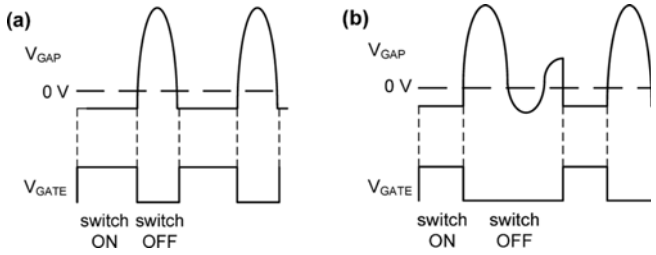

Fig. 5 Schematics of capacitor voltage (=gap voltage) (a) when the switch is turned on at the end of first half wave of oscillating voltage, (b) when the switch is turned on after the first half wave

Table 1 Experiment conditions

Tool	WC, Ø100 μm
Workpiece	WC, 200 μm thickness
Dielectric fluid	Deionized water
Positive voltage	80 V
R_1	17 Ω
R_2	4.7 Ω (100 Ω in case of 22 μH)
L	Cable inductance, 0.5, 4.5, 10, 22 μH
C	390 pF
Repetition frequency	1 MHz

4. Results and Discussion

Fig. 6 shows voltage pulses (open gap voltage) according to the inductance. As the inductance increases, the pulse width increases because the damped resonant frequency decreases according to Eq. (7). Thus, the absolute value of the negative voltage increases in order for zero average open gap voltage. In case of 22 μH, the absolute value of the negative voltage increased to more than 40 V. With large negative voltage and small R_2, a short current become high when the short occurs and the switch is turned on. The high short current can give damage to the circuit. Thus, R_2 = 100 Ω was used to achieve stable

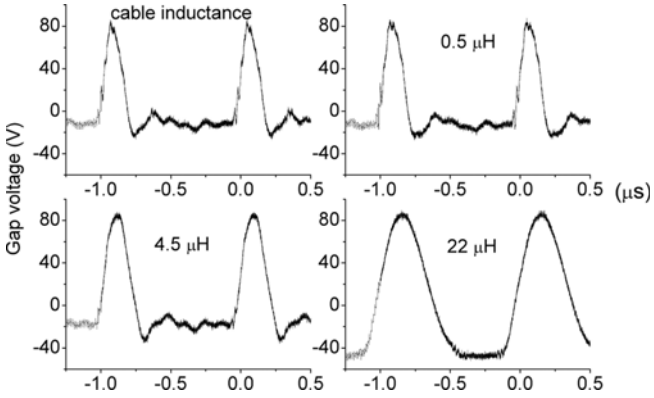

Fig. 6 Voltage pulses (open gap voltage) according to the inductance

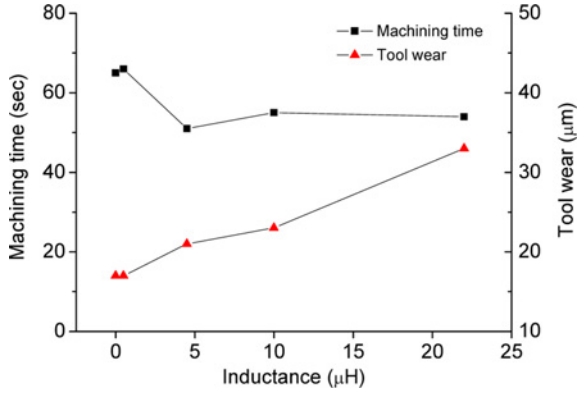

Fig. 7 Machining results according to the inductance (square denotes machining time and triangle denotes tool wear) (workpiece thickness: 200 μm)

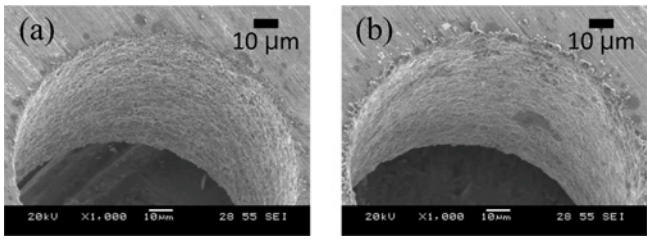

Fig. 8 Machined holes according to the inductance; (a) 0.5 μH (Ø118.5 μm), (b) 22 μH (Ø122.5 μm) (workpiece thickness: 100 μm)

short detection in the case of 22 μH.

Fig. 7 shows machining results. As the inductance increased, the machining time decreased and converged into the minimum machining time because of limited maximum feedrate. The tool wear increased according to inductance. Fig. 8 shows the machined holes with the inductance of 0.5 μH and 22 μH. In this case, a 100 μm thickness workpiece was used. In case of 22 μH, the rougher surface was observed and the hole size was slightly larger compared with that of 0.5 μH. The hole diameter for 0.5 μH and 22 μH was 118.5 μm and 122.5 μm respectively.

With a large inductance, it was observed that the positive peak voltage and the discharge current became higher after the discharge occurred as shown in Fig. 9. The positive peak voltage after discharges increased to almost 100, 130 and 180 V for 4.5, 10 and 22 μH, respectively. Therefore, the machining time decreased and the tool wear increased because of high discharge current.

Fig. 10 shows the capacitor voltage (=gap voltage) and the inductor current in case of 0.5 and 22 μH. T_1 and T_2 is the switch OFF and ON duration, respectively. During T_2 (switch ON), the inductor current increases with the time constant ($\tau = L/R_1$) according to the Eq. (3). With a large inductance, the inductor current increases slowly due to the large time constant. During T_1 (switch OFF), the voltage oscillates and forms the high positive voltage, and the inductor current also oscillates at the same time according to Eq. (8). The inductor current swings to the negative value at this time. When the discharge occurs during T_1, the inductor current, which is denoted by the circle in the Fig. 10, increases because the discharge current is provided to the machining gap. During T_2, right after the discharge, the inductor current increases by the time constant from this increased value formed at T_1. If the inductance is small, the inductor current increases rapidly to the steady state value during T_2 due to the small time constant. Therefore, the increase of the inductor current at the previous mode (T_1) does not affect the inductor current at this mode (T_2). In case of 0.5 μH, there is no difference of the inductance current during T_2 with or without the discharge as shown in Fig. 10(a). If the inductance is large, the inductor current cannot increase to the steady state value because of large time constant and shorter period of T_2 compared with small inductance. If the inductor current is increased at the end of T_1 due to discharge, the inductance current increases more during T_2 as shown in the Fig. 10(b) (long arrow). According to the Eqs. (6) and (10), the large inductor current at the end of T_2 increases the capacitor voltage during T_1. Therefore, in case of the large inductance, the voltage increases after the discharge.

5. Conclusions

In this work, effect of inductance was investigated in micro EDM using high frequency bipolar pulse generator used for electrolytic corrosion prevention in deionized water. As the inductance increased, voltage pulse width increased and absolute values of negative voltage increased. In the case of low inductance, constant discharge current was achieved. But, in the case of high inductance, the peak values of the gap voltage and discharge current have been fluctuated. With high

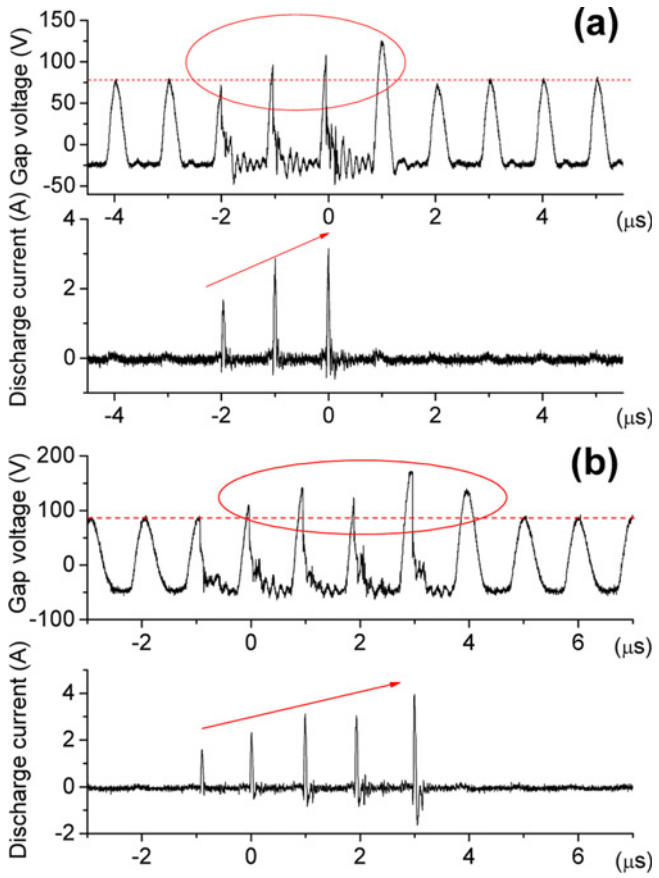

Fig. 9 Gap voltage and discharge current with (a) 10 μH, (b) 22 μH

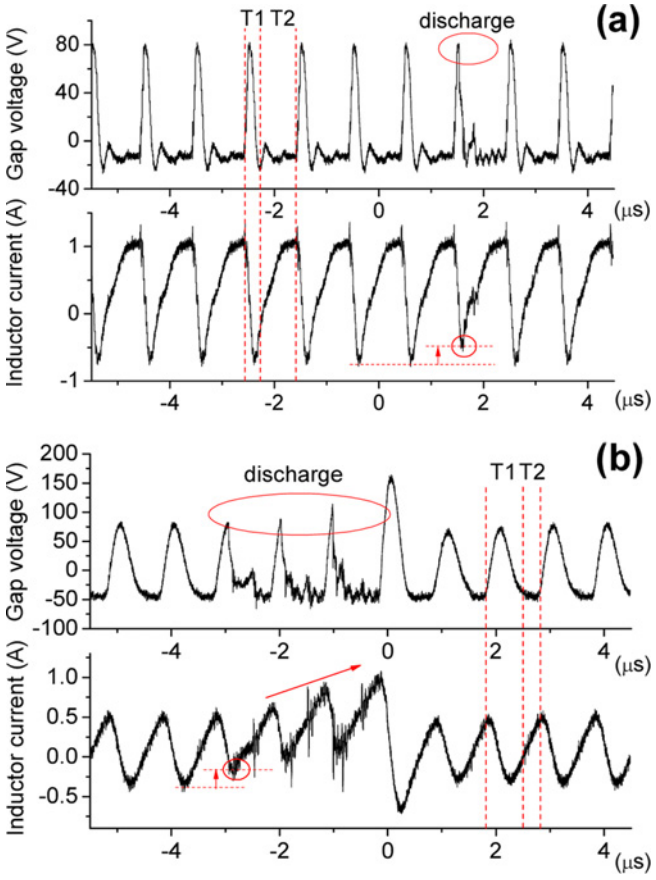

Fig. 10 Gap voltage and inductor curren with (a) 0.5 μH, (b) 22 μH

inductance, inductor current increased after discharge occurred. This increased inductor current also increased both capacitor voltage (=gap voltage) and discharge current. So, machining time decreased, and tool wear as well as side gap increased with high inductance. If discharge did not occur, the peak capacitor voltage became to 80V. However, the fluctuation of the peak voltage and current resulted in instability of gap distance and servo voltage. Thus, controllability was deteriorated. Moreover, at high inductance, the increased absolute value of the negative voltage resulted in high short current that could give damage to the circuit. In conclusion, low inductance guaranteed low tool wear, small side gap and fine surfaces with high controllability and stability. With high inductance, machining time decreased. But the controllability and the stability became deteriorated, and tool wear and side gap increased.

ACKNOWLEDGEMENT

This work was supported by Dongyang Mirae University research fund in 2014.

REFERENCES

1. Rajurkar, K., Levy, G., Malshe, A., Sundaram, M., McGeough, J., et al., “Micro and Nano Machining by Electro-Physical and Chemical Processes,” CIRP Annals-Manufacturing Technology, Vol. 55, No. 2, pp. 643-666, 2006.
2. Chu, W.-S., Kim, C.-S., Lee, H.-T., Choi, J.-O., Park, J.-I., et al., “Hybrid Manufacturing in Micro/Nano Scale: A Review,” Int. J. Precis. Eng. Manuf.-Green Tech., Vol. 1, No. 1, pp. 75-92, 2014.
3. Chung, D. K., Kim, B. H., and Chu, C. N., “Micro Electrical Discharge Milling Using Deionized Water as a Dielectric Fluid,” Journal of Micromechanics and Microengineering, Vol. 17, No. 5, pp. 867-874, 2007.
4. Song, K. Y., Chung, D. K., Park, M. S., and Chu, C. N., “Micro Electrical Discharge Drilling of Tungsten Carbide Using Deionized Water,” Journal of Micromechanics and Microengineering, Vol. 19, No. 4, Paper No. 045006, 2009.
5. Chung, D. K., Shin, H. S., Park, M. S., and Chu, C. N., “Machining Characteristics of Micro EDM in Water Using High Frequency Bipolar Pulse,” Int. J. Precis. Eng. Manuf., Vol. 12, No. 2, pp. 195-201, 2011.
6. Chung, D. K., Shin, H. S., and Chu, C. N., “Modeling and Experimental Investigation for Electrolytic Corrosion Prevention in High Frequency Micro EDM Using Deionized Water,” Microsystem Technologies, Vol. 18, No. 6, pp. 703-712, 2012.